ELSEVIER

Journal of Alloys and Compounds 434–435 (2007) 577–580

Journal of ALLOYS AND COMPOUNDS

www.elsevier.com/locate/jallcom

Evolution of nanoclusters at the coagulation of supersaturated solutions, a computer study

D.K. Belashchenko [a,*], E.S. Lobanov [a], G.F. Syrykh [b]

[a] *Moscow State Institute of Steel and Alloys, Moscow 119049, Russia*
[b] *Russian Research Center, Kurchatov Institute, Moscow 123182, Russia*

Available online 8 December 2006

Abstract

Molecular dynamics is used to investigate the coagulation of the precipitates in a supersaturated binary solution and its dependence on the thermodynamic properties of the system, concentration and temperature. Lennard–Jones potentials with different parameters for different pairs of atoms are employed. Coagulation proceeds by gradual growth of clusters and is not a thermally activated process. The rate of coagulation depends weakly on temperature. Solute clusters are initially amorphous and crystallize in the stable face-centered cubic structure only after reaching a specific size.

Keywords: Clusters; Amorphous materials; Nanostructures; Precipitation; Liquid quenching

1. Introduction

Crystallization of one-component liquids and coagulation of supersaturated solutions are very important stages of solid phase formation. At the initial stage of coagulation the particles have nanoscale dimensions. Crystallization of a one-component liquid is relatively well understood. The analytic solution for the size distribution of precipitates was considered [1–6]. The precipitation stage is followed by coalescence when smaller precipitates are dissolved and larger ones continue to grow [2,3,7]. The theory of coagulation of the solute from a supersaturated solution is less developed. Different stages of coagulation were considered analytically [6,7].

The conclusions of the thermodynamic theory were verified by numerical simulations of the solidification process. Crystallization of a one-component liquid with the Lennard–Jones interaction potential was investigated using the molecular dynamics (MD) method [8–14]. Face-centered cubic (FCC) structure is stable with this potential. In some cases [9,11] the precipitates with the metastable body-centered cubic (BCC) structure were detected.

In this paper we study the initial stages of solute coagulation in a supersaturated binary solution using the MD method. The interaction potentials must produce positive deviations from ideality for the liquid. When the system is cooled down into the two-phase region of the phase diagram, the second phase coagulates in the form of precipitates, or clusters.

2. Simulation

We used Lennard–Jones interaction potentials:

$$u_{ij}(r) = 4\varepsilon_{ij}\left[\left(\frac{r_0}{r}\right)^{12} - \left(\frac{r_0}{r}\right)^{6}\right] \quad (1)$$

For all atom pairs (11, 12 and 22) we put $r_0 = 2.27$ Å; further, we assumed $\varepsilon_{11} = 0.070$ eV, $\varepsilon_{22} = 0.174$ eV, and the parameter ε_{12} was assigned different values of 0.122, 0.100, 0.089 or 0.078 eV. In these cases the mixing energy $\Delta\varepsilon = -\varepsilon_{12} + (\varepsilon_{11} + \varepsilon_{22})/2$ is equal to 0.000, 0.022, 0.033 or 0.044 eV. For $\Delta\varepsilon > 0$ the solution shows positive deviations from ideality and separates in two liquid phases at low temperatures. Positive deviations from ideality increase with $\Delta\varepsilon$. The models contained $N = 2997$ or 5997 atoms in the simulation cube with periodic boundary conditions. The numbers of solute atoms were $N_2 = 50$, 100, 200, 400 or 800.

The simulations were performed using the Verlet algorithm. The time step was equal to $0.01\tau_0$ or $0.03\tau_0$, where τ_0 is the internal time unit. For example, for argon $\tau_0 = 6.434 \times 10^{-14}$ s. The MD run length was generally of the order of 10^5 time steps,

* Corresponding author.
E-mail address: dkbel@mail.ru (D.K. Belashchenko).

0925-8388/$ – see front matter © 2006 Published by Elsevier B.V.
doi:10.1016/j.jallcom.2006.08.196

but in some cases it exceeded 1 million steps. Constant temperature (500, 600 or 800 K) and zero pressure were maintained in the simulations. We analyzed the coagulation process by detecting clusters of solute atoms (each atom belonging to a cluster must have at least one neighbor in this cluster). Crystallization of clusters can be observed either visually or by analyzing the structure factor of solute atoms $S(\mathbf{q})$:

$$S(\mathbf{q}) = \left| \frac{1}{N_2} \sum_j \mathrm{e}^{-\mathrm{i}\mathbf{q}\mathbf{R}_j} \right|^2 \quad (2)$$

Here N_2 is the number of solute atoms, $\mathbf{q}$ the scattering vector, and $\mathbf{R}_j$ the coordinate of the jth atom. If the atoms form an ideal crystal lattice, then the structure factor $S(\mathbf{q})$ must be equal to unity in the directions of reciprocal lattice vectors and zero in other directions. If the system consists of crystalline clusters surrounded by the liquid, the $S(\mathbf{q})$ values are less than unity and are of the order of 0.1 [15].

2.1. Phase diagram analysis

In the case of a system with the potential (1) the triple point temperature is $T_{T*} = kT_T/\varepsilon = 0.68 \pm 0.02$ [16] (k is the Boltzmann constant). For argon $\varepsilon = 0.0103$ eV and $\varepsilon/k = 119.8$ K; its melting point (at 68.9 kPa) is 83.8 K. Using the value $T_{T*} = 0.68$ we obtain the melting point of 553 K at $\varepsilon = 0.070$ eV and 1374 K at $\varepsilon = 0.174$. These were the melting points of two components (solvent and solute).

We calculated the phase diagram of the binary system at three values of ε_{12}. In the case $\Delta\varepsilon = 0.022$ eV we obtain a wide two-phase region (solvent-reach liquid plus solute-reach solid) with the critical point near 1920 K. For $\Delta\varepsilon = 0.044$ eV the critical point is near 3840 K. At 600 K and $\Delta\varepsilon = 0.044$ eV the solubility of solute in the liquid is near 0.97 mol%. As $\Delta\varepsilon$ grows the equilibrium solubility diminishes.

2.2. The coagulation process

This process was simulated for the total number of atoms $N = 2997$ at temperatures 500, 600 and 800 K. Cooling of the solution with 1.67–13.3 at.% (50–400 solute atoms) from 2000 to 600–800 K takes it into two-phase region and triggers the coagulation of the solute.

The initial states were taken from MD models created with $\varepsilon_{12} = 0.122$ eV at the temperatures 500, 600, 800 and 2000 K. Then the parameter ε_{12} was changed to 0.100, 0.89, 0.78 or 0.56 eV, and the behavior of the system was investigated in long MD runs. In the case of full coagulation all solute particles gather in one cluster and only small particles remain in the liquid phase. The precipitating clusters are amorphous. We monitored the coagulation process using the total interaction energy U_{22} of the solute–solute pairs and the distribution of solute clusters.

During the coagulation process the solute atoms approach each other and their interaction energy diminishes. This energy asymptotically approaches a definite minimal value. A special feature of the $U_{22}(t)$ graph is the presence of sharp kinks on the background of smoothly diminishing energy U_{22}. These jumps appear when two neighboring solute clusters attract each other and form a cluster.

Another way to monitor coagulation is to analyze the distribution of solute clusters. For example, the notation $1^{15}2^{10}8^{2}98^{1}$ means that the system contains 15 isolated solute atoms (monomers), 10 dimers, two 8-atom clusters, and one large cluster with 98 solute atoms.

Dependence of the coagulation rate on solute concentration was considered. The observed dependence of U_{22} on time t may be approximated as $\ln y = -kt + \ln(y_0)$ where $y(t) = (U_{22}(t) - U_{22}^{\infty})/(N_2 - N_{20})$ and U_{22}^{∞} is the asymptotic value of $U_{22}(t)$ at $t \to \infty$. This dependence is almost linear. The slope enhances with the growth of N_2. The coagulation rate grows linearly in the number of solute atoms per unit volume, because the rate of cluster collisions increases with their density.

One can explore the coagulation process using the cluster distribution. A convenient characteristic here is the value of the second moment of the cluster size distribution $M_2 = \sum i^2 \nu(i)/N_2$, where $\nu(i)$ is the number of clusters containing i atoms. The dependence of M_2 on time for $N = 2997$, $T = 600$ K, $\Delta\varepsilon = 0.044$ eV and $N_2 = 100$ is shown in Fig. 1. Sharp upturns happen when two clusters coalesce; downturns correspond to the opposite events. The graphs for $N_2 = 50$, 200 and 400 are similar. The initial slopes are proportional to N_2^2. In real time the graphs very quickly approach the asymptotic values. For example, at $N_2 = 100$ this time is equal to 3.6×10^{-10} s (for argon). It diminishes with the growth of the solute atom number, i.e. with the growth of supersaturation.

Let us consider some cluster distributions after long MD runs. For example, at 600 K, $N = 2997$ and $N_2 = 200$ after 250,000–460,000 time steps (i.e. at $t/\tau_0 = 2500$–4600) the distributions are as follows:

$\Delta\varepsilon$ (eV)	Distribution
0.022	$1^{24}2^{5}3^{4}4^{1}5^{1}6^{1}18^{1}19^{1}23^{1}35^{1}44^{1}$
0.033	$1^{18}2^{2}4^{1}6^{1}10^{1}12^{1}15^{1}26^{2}79^{1}$
0.044	$1^{6}3^{1}58^{1}133^{1}$
0.066	$9^{1}84^{1}107^{1}$

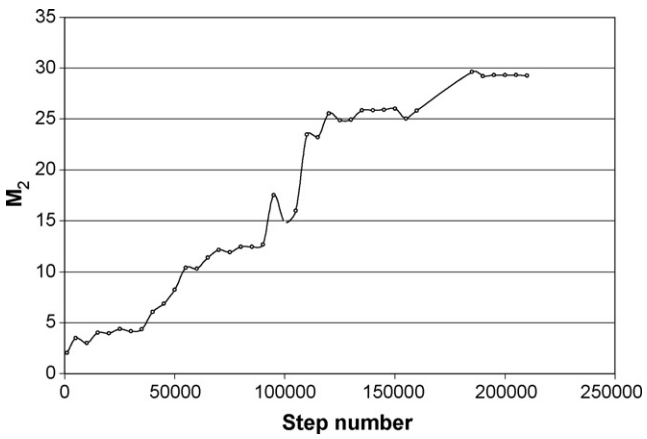

Fig. 1. Dependence of the second moment M_2 on step number for the case $N = 2997$, $T = 600$ K, $\Delta\varepsilon = 0.044$ eV and $N_2 = 100$. The length of time step is equal to $0.03\tau_0 = 1.93 \times 10^{-15}$ s.

At $\Delta\varepsilon = 0.022$ eV the system is obviously far from equilibrium. The coagulation rate grows quickly with the value $\Delta\varepsilon$, and for $\Delta\varepsilon = 0.066$ eV it generally takes about 400,000 steps to reach equilibrium.

In the case $N = 2997$, $T = 600$ K and $\Delta\varepsilon = 0.044$ eV we obtained the following distributions of solute clusters:

N_2	Step number	Distribution
50	315,000	$1^8 2^1 12^1 13^1 15^1$
100	210,000	$1^8 3^1 19^1 28^1 42^1$
200	140,000	$1^6 3^1 58^1 133^1$
400	100,000	$1^2 398^1$

At $N_2 = 400$ almost all solute atoms coagulate in one cluster. The cluster distribution is very sensitive to the initial conditions, but the values of energy U_{22} in these cases are rather close.

Next, dependence of the coagulation rate on system size was considered. Besides the models of the size $N = 2997$ the coagulation of solute in the system of the size $N = 5997$ particles (800 solute atoms) was investigated at 600 K and $\Delta\varepsilon = 0.044$ eV. The concentration here is equal to the case of $N = 2997$ and $N_2 = 400$. The ratio of U_{22} values for greater and lesser models was 1.86–1.91 along the run of 275,000 time steps and is very near to the ratio of solute atom numbers (=2). So the result (in respect to one solute atom) depends too little on the system size.

The cluster distributions are less reproducible. The coagulation of small groups in greater ones, containing some tens of atoms, goes with similar rates in models with equal N_2. Firstly monomers and small groups disappear. It takes about 100,000 time steps. Further big clusters steadily attract themselves and joined together. This stage is far longer.

For the dependence of coagulation rate on the temperature, data were obtained at three temperatures 500, 600 and 800 K. The time dependences of energy U_{22} are shown in Fig. 2 for $N = 2997$, $N_2 = 200$ and $\Delta\varepsilon = 0.044$ eV. The temperature has almost no effect on the coagulation rate which is very low, and even at $t/\tau_0 \sim 2500$ the process is still in the initial (linear) part of the trajectory. The data for $N_2 = 200$ and $\Delta\varepsilon = 0.033$ eV are similar. Heating from 500 to 800 K leads to a very small increase in the coagulation rate by 12–15% at intermediate and later stages, and by about two times at the initial stage. The kinetic analysis is not straightforward because the solute solubility N_{20} in the liquid phase decreases with the growth of $\Delta\varepsilon$ and at cooling. In fact, at $\Delta\varepsilon = 0.022$ eV the heating lowers the coagulation rate, at $\Delta\varepsilon = 0.033$ eV temperature has almost no effect on the rate, and at $\Delta\varepsilon = 0.044$ eV the rate grows slightly with temperature. These results can be explained by the diminishing of the solute solubility with the growth of $\Delta\varepsilon$. At $\Delta\varepsilon = 0.022$ eV the solubility is rather large, and the main role of heating is to lower the supersaturation as the liquidus line is approached. At $\Delta\varepsilon = 0.044$ eV the solubility is low and depends weakly on temperature, so the main effect of heating is to increase the diffusion rate. At $\Delta\varepsilon = 0.033$ eV these effects compensate each other.

At the initial stages the growth of the diffusion rate plays the main role in accelerating the coagulation rate at heating. On more advanced stages the lowering of supersaturation becomes important. However, the effect of temperature is strongly masked by variations in the coagulation process related to the randomness of cluster formation and decay.

Therefore we see that the growth of diffusivity at heating does not lead to a proportional enhancement of the coagulation rate. Hence the transport of atoms to the surface of existing clusters is not the bottleneck. At the initial stages the coagulation is limited by the attachment of small clusters (monomers and dimers) to larger clusters. These events occur by the removal of solvent atoms from the space between the boundaries of solute clusters. Weak temperature dependence indicates that the cluster growth is not the thermally activated process.

Dependence of the coagulation rate at $N = 2997$, $N_2 = 200$, $T = 500$ K on $\Delta\varepsilon$ value is shown in Fig. 3. The graphs for 600 and 800 K are similar. Solubility in the solid phase diminishes with the growth of $\Delta\varepsilon$. Supersaturation ζ is equal to the ratio of solute concentration X_2 to the equilibrium one X_{2s} with respect to the solid solute phase. "The driving force" of coagulation is the difference between the chemical potentials of solute atom in the solution and in the solid phase $f = kT \ln \zeta$. In the case of small solubility the theory of regular solutions gives $NkT \ln X_{2s} \cong -Nz\Delta\varepsilon$ and $f \cong kT \ln X_2 + z\Delta\varepsilon$ (z is the coordination number). Hence the growth of $\Delta\varepsilon$ must lead to the enhancement of the coagulation rate, as it is seen in Fig. 3.

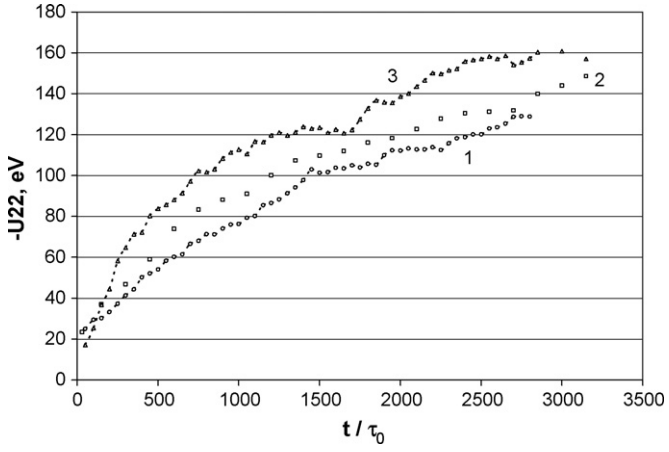

Fig. 2. Time dependence of U_{22} at different temperatures. $N = 2997$, $N_2 = 200$ and $\Delta\varepsilon = 0.033$ eV: (1) 500 K, (2) 600 K, and (3) 800 K.

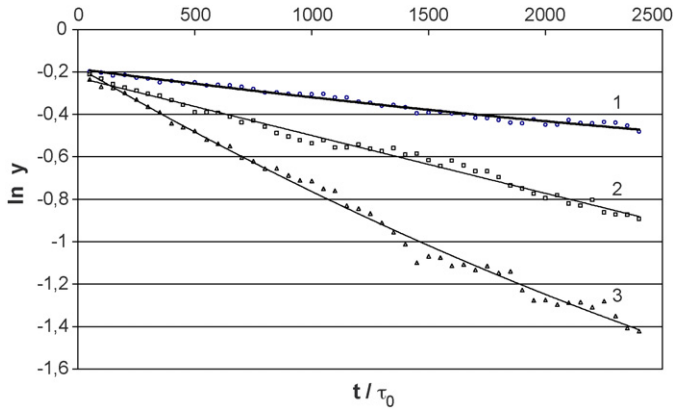

Fig. 3. Time dependence of $\ln y$ at 500 K and different values $\Delta\varepsilon$. In all cases $N = 2997$, $N_2 = 200$. The values of $\Delta\varepsilon$ are equal to: (1) 0.022 eV, (2) 0.033 eV, and (3) 0.044 eV.

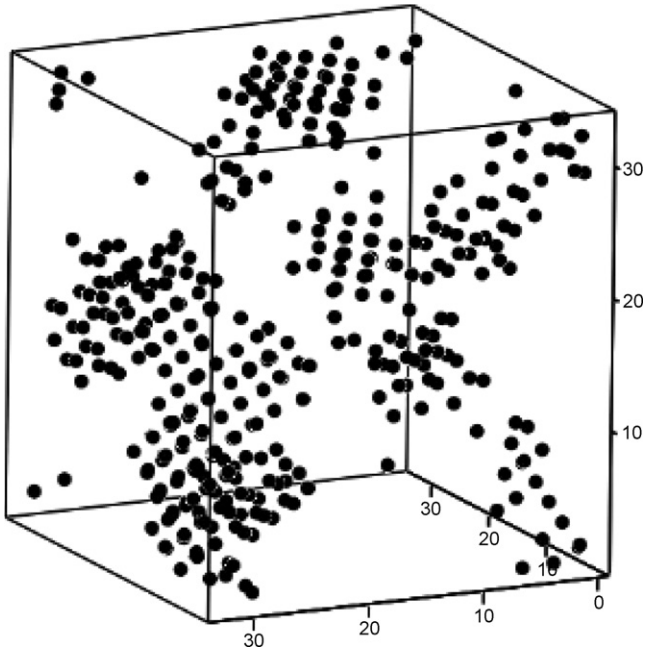

Fig. 4. Visualization of solute atoms in the model with $N_2 = 400$ and $\Delta\varepsilon = 0.022$ eV. Relaxation time $t = 16{,}577\tau_0$. The solvent atoms are not shown.

In sufficiently long MD runs (of the order of 10^4 to 10^5 τ_0) great amorphous clusters existing in the supersaturated solution may crystallize. This process can be observed either visually or by calculating the structure factors (SF) $S(\mathbf{q})$ for different directions of the scattering vector. The formation of ordered atomic layers was visually observed in the models with $N = 2997$, $N_2 = 400$, 200, 100 at $\Delta\varepsilon = 0.022$ eV and $N = 2997$, $N_2 = 400$ at $\Delta\varepsilon = 0.044$ eV and also in the model with $N = 5997$, $N_2 = 800$ and $\Delta\varepsilon = 0.044$ eV. In the last case the maximal value of SF was equal to 0.0158 for a solvent and 0.0707 for solute clusters. The smallest crystal precipitate contained 67 atoms; it was discovered in the model with $N = 2997$, $N_2 = 100$ and $\Delta\varepsilon = 0.022$ eV. In the models with too few solute atoms the calculation of SF is less informative, because too few atoms contribute to the sum.

The crystal clusters appearing in the model may be directly observed. In this case the atomic rows and layers are clearly seen. One such situation is shown in Fig. 4 (model with $N = 2997$, $N_2 = 400$ and $\Delta\varepsilon = 0.022$ eV after the relaxation time $16{,}577\tau_0$).

In the model with $N = 5997$, $N_2 = 800$ and $\Delta\varepsilon = 0.044$ eV (basic cube edge length 43.850 Å) after the long run at 600 K the cluster distribution was obtained as $82^1112^1201^1405^1$. Taking the cluster form as spherical one can evaluate the total boundary surface as 3340 Å^2. Dividing the energy difference by this surface we obtain the excess surface energy 0.515 J/m^2. This value is probably highly overestimated because of the presence of numerous defects in solute clusters and their irregular shape.

3. Discussion

In the case of coagulation of a binary solution with the potentials (1) it is not necessary to overcome the potential barriers of noticeable heights, and therefore the process proceeds without thermal activation. As a result, temperature has a very weak effect on the coagulation rate.

The initial stage of coagulation proceeds rather quickly in real time and takes about 10^{-9} s. At later stages the distance between clusters grows, and the coagulation rate diminishes. Our models are too small to study these later stages of coagulation.

The coagulation mechanism consists in the attachment of monomers and small clusters to larger ones. When a cluster grows beyond a certain size, it may crystallize. Crystallization of amorphous clusters in our models was observed in all cases when the cluster size exceeded 60–70 atoms. A similar (two-stage) feature was observed in Ref. [17] in the simulation of globular proteins.

Acknowledgements

The work was conducted under the financial support of Russian Fond of Fundamental Studies (Grant No. 03-02-16803a), Scientific School (SS 2037. 2003.2) and a program "Neutron Study of Condensed Matter."

References

[1] Ja.B. Zeldovich, JETP 12 (1942) 525–532 (in Russia).
[2] I.M. Lifshitz, V.V. Slezov, JETP 35 (1958) 479–492 (in Russia).
[3] E.M. Lifshitz, L.P. Pitajevskij, Physical kinetics, Science, Moscow, 1979 (in Russia).
[4] F.M. Kuni, A.P. Grinin, Colloid J. 46 (1984) 460–466 (in Russia).
[5] F.M. Kuni, A.P. Grinin, Theor. Math. Phys. 80 (1989) 418–425 (in Russia).
[6] V.V. Slezov, Ju.P. Shmelzer, Fiz. Tverdogo Tela. 43 (2001) 1101–1112 (in Russia).
[7] V.V. Slezov, Theory of Diffusive Decomposition of Solids Solution. Sov. Scientific Reviews, vol. 117, Moskow, 1995.
[8] C.S. Hsu, A. Rahman, J. Chem. Phys. 71 (1979) 4974–4986.
[9] P.R. ten Wolde, M.J. Ruiz-Montero, D. Frenkel, J. Chem. Phys. 104 (1996) 9932–9947.
[10] M.J. Mandell, J.P. McTague, A. Rahman, J. Chem. Phys. 64 (1976) 3699–3702.
[11] M.J. Mandell, J.P. McTague, A. Rahman, J. Chem. Phys. 66 (1977) 3070–3075.
[12] R.D. Mountain, A.C. Brown, J. Chem. Phys. 80 (1984) 2730–2737.
[13] J. Yang, H. Gould, W. Klein, Phys. Rev. Lett. 60 (1988) 2665–2670.
[14] W.C. Swope, H.C. Andersen, Phys. Rev. B 41 (1990) 7042–7049.
[15] D.K. Belashchenko, R.N. Pavlov, Russ. J. Phys. Chem. 78 (2004) 1777–1784.
[16] J.-P. Hansen, L. Verlet, Phys. Rev. 184 (1969) 151–161.
[17] W. Hu, D. Frenkel, V.B.F. Mathot, Macromolecules 36 (2003) 8178–8183.